Transportation Engineering 2 (2020) 100010

Contents lists available at ScienceDirect

Transportation Engineering

journal homepage: www.elsevier.com/locate/treng

Adaptive design of a universal automotive ball joint separating device

Christian Emeka Okafor*, Okpa Omena Oghenemaero, Modebelu Chukwuebuka, Osinachi Odeke Isaac

Department of Mechanical Engineering, Nnamdi Azikiwe University, Awka, Nigeria

ARTICLE INFO

Keywords:
Adaptive design
Automotive ball joint separator
Wheel hubs
Control arms
Optimization
Response surface methodology
Mechanical advantage

ABSTRACT

Ball joint provides universal pivoting movement between the wheel hubs and control arms. The use of conventional ball joint separators was marred by cracks, damage to the castle nut on the joint stud and inferior mechanical advantage. An adaptive design was therefore necessary in response to these performance deficits and reiterated failures. The objective of this study was to offer the design and production of a universal ball joint separating device. GRANTA Selector was utilised in new material search. Design process was realized through ANSYS finite element analysis and structural stress analysis was performed using a load range of 200–1400 N. Optimal conditions of effort arm (mm) = 67.50, load arm (mm) = 66.38 and pitch (mm) = 2.50 were obtained at Mechanical Advantage (MA) of 0.85 giving an overall device efficiency of 83.51%. The maximum stress and maximum deformation respectively occurred close to the pivot at the base of the bottom half and at the tip of the top part of the ball joint separator. So, it was concluded that the effects of the control variables and their optimization were regarded as very useful to ascertain the optimum mechanical advantage of the device. The stress however is less than the yield strength of high carbon steel selected for device production and the separator performed the required tasks without failure.

1. Introduction

Automobile ball joints function like hinges and connect the suspension control arms to the steering knuckles with a rotating spherical stud and a socket, giving the wheels a wide range of movement; consequently most vehicles use ball joints to maintain the relative position between constitutive elements [1]. It is a rotating and swivelling element that is typically installed at the interface between two parts. Ball joint as shown in Fig. 1 do not feature a disassembly possibility which means that it cannot be repaired but can only be replaced [2–4]. Although various designs such as the pickle fork, simple claw-type press and ball joint press have been made for the separation of the ball joint from the steering knuckles in a vehicle, such designs were marred by cracks from a small number of near-yield overloads, damage to the castle nut on the joint stud and inferior mechanical advantage. The ball joint separator is of utmost importance in the field of automobile study because it has a whole lot of relevance in motor servicing and maintenance [3]; effective use of the device can minimise recurrent damages to steering knuckle and rubber boot of the ball joint arising from the utilization of traditional means of ball joint removal [2].

This study was initiated as a consequence of the researchers' discussions with local automotive mechanics which found the existing pickle fork, simple claw-type press, ball joint press and cast iron ball joint separators wavering for a wide range of car models and their subsequent resort to the use of hammer on suspension control arm as a means of removing failed ball joints. Considering the critical role of ball joints in providing universal pivoting movement between the wheel hubs and control arms, an adaptive development of a universal ball joint separator is essential for easy removal of the ball joint from the steering knuckle in cars, minivan, small SUV and all terrain vehicles. Adaptive design as illustrated in Fig. 2 is the process in which the parameters of the existing design or engineering device is slightly modified to improve quality, incorporate user need or suit a new trend in the market. McMahon and Draper [5] sees adaptive design as evolving in response to changes in the "demands" placed on the existing design by the end-users and within limitations imposed by "constraints" which arise from the environment in which the design exists.

For efficient adaptive design, related design models, stakeholder and user experience gathered from the existing product trial is usually adopted to inform design improvements of a re-engineered technology. The deployment of adaptive design strategies in retrofitting existing technologies for improved scope of application and efficiency have been reported [6–12]. Additionally, scholarly evidence has shown that adaptive design is most times combined with other product development strategies for optimal performance [13–15]. A general structure of an adaptive design scheme during a conceptual phase of functional device design as shown in Fig. 2 also involves adaptation of an existing design

* Corresponding author.
E-mail address: ce.okafor@unizik.edu.ng (C.E. Okafor).

https://doi.org/10.1016/j.treng.2020.100010
Received 21 April 2020; Received in revised form 30 May 2020; Accepted 26 June 2020

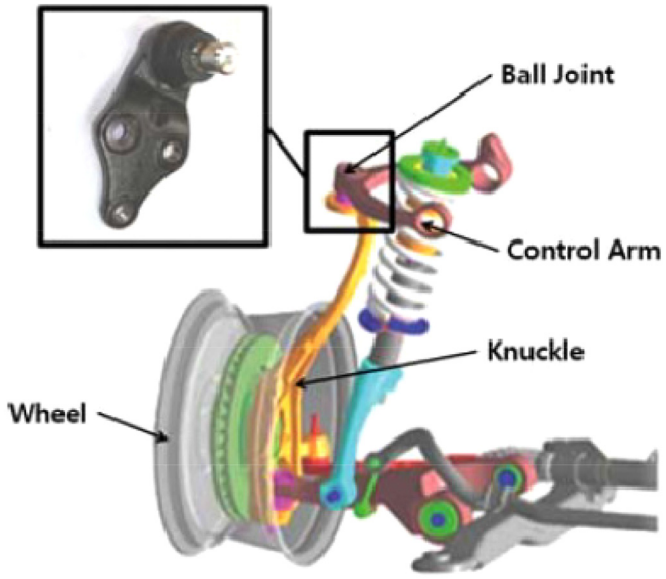

Fig. 1. Location of a ball joint [4].

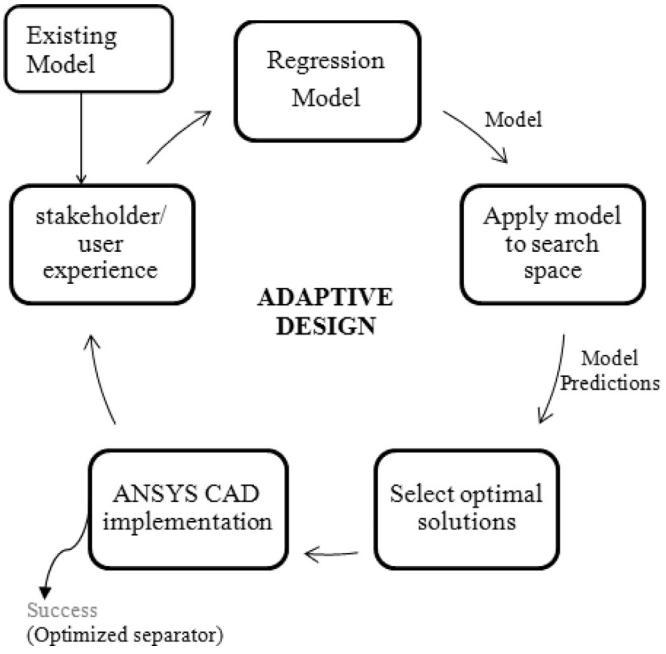

Fig. 2. Adaptive design strategy.

model to meet the performance specification of the desired device [9]. Ramos, Melgosa and Castrillo [16] appraised the importance of adaptive expertise in a Computer Aided Design environment to ensure that the design intent is not compromised. Irsel [17] applied computer aided adaptive system design with engineering manufacturing and concludes that CAD implementation has a shorter production time and lower costs. Besides cost, resistance and weight, there are too many design parameters to be evaluated and considering too many design parameters will bring along too many solutions. Thus, it will be wise to use an optimum design in the analysis to achieve the desired goal [18]. In the present study, the ANSYS computer aided design and Central Composite Design were combined for the purpose of attaining optimum factor setting and improved target response.

The ball joint separator considered was conceptualized as a class 1 lever consisting of an upper half beam pivoted at the fulcrum which is capable of transmitting torque that provides the necessary mechanical advantage. Arup [19] utilised adaptive design on crank and slotted lever mechanism to incorporate the class 1 lever instead of the usual 3 lever. Similarly, Jagdish, Poonam and Kedar [20] designed and fabricated a lever operated wheelchair and arrived at a mechanism that requires less effort by an operator to operate. Other applications of lever mechanism in mechanical system include mastication force analysis on the fulcrum point of first class lever by [21] and toggle lever caliper cable trolley brake by [22]. These studies suggest that lever mechanism can be designed to magnify the force applied to an object so that work can be done efficiently and effectively.

However, apart from a recent study by Muscă, Rômânu and Gagea [1] on preliminary assessment of friction in automotive ball joints, there is limited published research evidence on universal automotive ball joint separator design, a gap that is filled by the present study. Therefore the present study undertook adaptive design of ball joint separating device with a firm grip to its known and established lever working principles while adapting the embodiment to change material requirements and optimise mechanical advantage.

2. Materials and methods

The ball joint separator having top half and bottom half assembly follows a simple lever mechanism in which the top half is hinged at the centre. The various designations are P as effort applied due to the screwing effect on the top half, W as load arising from the ball joint, a as length of the effort arm and b as length of the load arm. The moments about the fulcrum on both sides of the lever are equal and can be expressed as:

$$\frac{W}{P} = \frac{a}{b}\ (1) \tag{1}$$

The terms $\frac{W}{P}$ and $\frac{a}{b}$ are known as the mechanical advantage and leverage of the device. The efforts required to produce the force is calculated by considering bolt tightening. To obtain a greater mechanical advantage in order to separate the ball joint, a screw is needed to change an angular motion into linear motion in such a way that a torque is applied to the screws, thus, creating an axial force. Schmid et al. [23] reported that lead angle (α) relates the thread pitch to the pitch circumference in the order of Eq. (2):

$$\alpha = \ tan^{-1}\left(\frac{p}{\pi d_p}\right) \tag{2}$$

where d_p is the pitch diameter, and p is the thread pitch. To determine the effort P required moving the load W, it is necessary to observe the forces acting on a screw thread. The net force on the threads is represented by a single statically equivalent force P_n.

$$P_n = \frac{W}{cos\theta_n cos\alpha - \ \mu\ sin\alpha} \tag{3}$$

where μ represents the thread coefficient of friction for properly greased and the angle θ_n is given as

$$\theta_n = \ tan^{-1}\left[cos\alpha\ tan\left(\frac{\beta}{2}\right)\right] \tag{4}$$

Also the torque required to raise the load is

$$T = W\left[\frac{\left(\frac{d_p}{2}\right)\left(cos\theta_n tan\alpha + \mu\right)}{cos\theta_n - \ \mu\ tan\alpha}\right] \tag{5}$$

where α is the lead angle, β is the thread angle and μ is the coefficient of friction between the thread. The short-form equation which describes the relationship between applied torque and the tension created is described by [24] as:

$$T = W(k \times d) \tag{6}$$

where k = nut factor, sometimes called the friction factor and d = bolt diameter. Combining Eqs. (6) and (5) shows that the nut factor is dependent on friction coefficients and thread geometry parameters. However, as the thread geometric parameters are determined for a standard bolt, the friction coefficient becomes the dominant factor affecting the nut factor. The efficiency of a screw mechanism (e_s) is the ratio of work output to work input as shown in Eq. (7) while the efficiency of the device (e_d) is as shown in Eq. (8)

$$e_s = \frac{Wl}{2\pi T_r} \times 100\% \tag{7}$$

$$e_d = \left(\frac{W}{P}\right) \times \left(\frac{b}{a}\right) \times 100\% \tag{8}$$

The area of bolt under load engagement situation was proposed by [25] as

$$\text{Stress Area} = \frac{\pi}{4} \times \left(\frac{d_p + d_c}{2}\right)^2 \tag{9}$$

Compressing stress S_c which is the value of the stress between the threads that combine to transfer the needed force to the ball joint through the separator top half was determined following Eq. (10).

$$S_c = \frac{P}{\pi\left(d^2 - d_c^2\right)n} \tag{10}$$

where:

d_p= Pitch diameter = 10.863(mm),
d_c = Core or minor diameter = 10.106(mm),
d = Major diameter (mm),
d_c = Minor diameter (mm)
n = Number of threads in engagement and
P = Maximum safe axial load (N).

2.1. Material selection requirements

To develop an optimal product, designers need to couple optimal design with optimal materials selection. Material selection is essentially valuable in engineering enterprises for optimal utilization of vital material data and for smart decisions across product design and development. The upper half of the universal ball joint separator was considered as a light beam loaded in bending which must meet a constraint on its stiffness S, meaning that it must not deflect more than δ under a load F. Ashby and Cebon [26] derived an expression for minimization of mass in a loaded beam as

$$m \geq \left(\frac{12S}{C_1 L}\right)^{12} (L^3)\left(\frac{\rho}{E^{1/2}}\right) \tag{11}$$

It follows that the best material for a light stiff ball joint separator are those with the smallest value of $(\frac{\rho}{E^{1/2}})$, this can be inverted for large values of material index with respect to stiffness [26] in Eq. (12) and with respect to strength [27] in Eq. (13).

$$M = \frac{E^{1/2}}{\rho} \tag{12}$$

$$M = \frac{\sigma_y{}^{1/2}}{\rho} \tag{13}$$

where σ_y = strength of material, ρ = density of material, E = Modulus of elasticity of material.

2.2. Statistical analysis

The ANSYS Computer aided design and Central Composite Design were used to assess the values of the effort arm, load arm and thread pitch for the attainment of optimal mechanical advantage. Central Composite Design of response surface methodology involves varying the effort arm (mm) from 55.50 to 67.50, load arm (mm) from 66.38 to 70.50 and thread pitch (mm) from 2.50 to 3.00. The response surface appeared wrapped due to the curved nature which justified ascent to a higher degree polynomial; hence, the data acquired were fitted to the empirical second-order regression model of Eq. (14).

$$Y = \beta_0 + \sum_{i=1}^{k} \beta_i x_i + \sum_{i=1}^{k} \beta_{ii} x_i^2 + \sum_{i=1}^{k-1} \sum_{j}^{k} \beta_{ij} x_i x_j + \varepsilon \tag{14}$$

where Y is response; β_0,β_i (i = 1, 2,.....k) and β_{ij} (i = 1, 2,...k; j = 1, 2,...k) are the model coefficients; x_i and x_j are the coded independent variables. Also, the adequacy of the model was checked using the coefficient of determination (R^2), adjusted R^2 and predicted R^2 values. The interactive effects of the independent variables (effort arm, load arm and pitch) on the dependent variable (mechanical advantage) were examined using the analysis of variance (ANOVA). ANOVA is a statistical test for detecting differences in group means as there is one parametric dependent variable and three independent variables.

2.3. Computer Aided Design implementation protocol

In a bid to improve the design quality, the ANSYS CAD implementation in Fig. 3 was carried out as an overlay on the six phases of design process defined by [30]. Geometric modelling was conducted in SolidWorks® which permits the use of the CAD system in creating geometric models of universal ball joint separator from basic building blocks available in the system. Engineering analysis which takes the form of Finite Element Analysis of the model was carried out using ANSYS 15.0. Then design evaluation in terms of dimensioning and error checking was done to review accuracy and consistency of model dimensions. Finally the detailed engineering drawing was carried out and reported.

3. Results and discussion

3.1. Analysis of variance (ANOVA)

Results from the Analysis of Variance (ANOVA) for the quadratic model is presented in Table 1, The Model F-value of 13,111,664.59 implies that the model is significant. There is only a 0.01% chance that an F-value this large could occur due to noise. P-values less than 0.05 indicate that model terms are significant. In this case A, B, C, AB, AC, A^2, B^2, C^2 are significant model terms. Values greater than 0.10 indicates that the model terms are not significant.

The Predicted R^2 of 1.00 is in reasonable agreement with the Adjusted R^2 of 1.00; i.e. the difference is less than 0.2. Adeq Precision measures the signal to noise ratio. A ratio greater than 4 is desirable. The ratio of 13,351.08 indicates an adequate signal. This model can be used to navigate the design space. Eq. (15) is the specific case of the general predictive equation derived for individual investigations from the multivariate regression analyses implemented on the Design expert.

$$\begin{aligned}\text{MechanicalAdvantage} = {} & \\ & +0.884991 \\ & +0.029507\,\text{Effort arm} \\ & -0.026223\ \text{Load arm} \\ & +0.003064\ \text{Pitch} \\ & -0.000214\,\text{Effort arm} * \text{Loadarm} \\ & -0.000034\ \text{Effort arm} * \text{Pitch} \\ & -1.65767\text{E}-06\,\text{Load arm} * \text{Pitch} \\ & -1.36052\text{E}-06\,\text{Effort arm}^2 \\ & +0.000192\,\text{Load arm}^2 \\ & -0.000165\ \text{Pitch}^2\end{aligned} \tag{15}$$

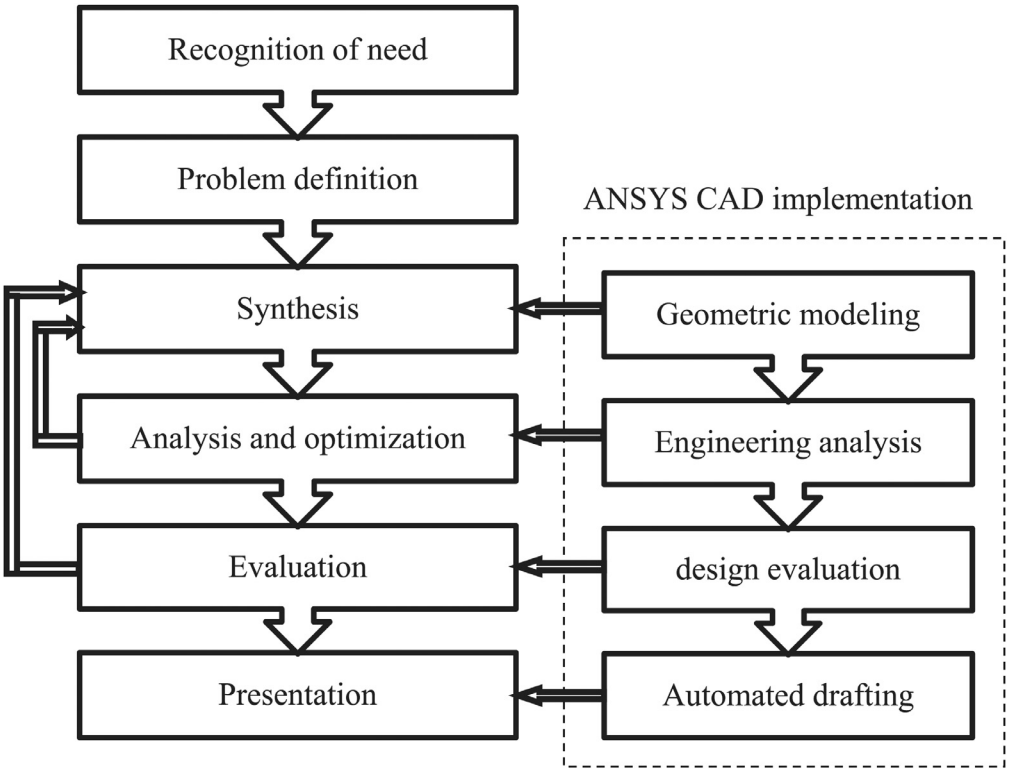

Fig. 3. ANSYS CAD implementation protocol for universal ball joint separator.

Table 1
Analysis of Variance (ANOVA) for quadratic model.

Source	Sum of Squares	df	Mean Square	*F*-value	*p*-value	
Model	0.1152	9	0.0128	1.311E+07	< 0.0001	significant
A-Effort arm	0.0073	1	0.0073	7.480E+06	< 0.0001	
B-Load arm	0.0053	1	0.0053	5.476E+06	< 0.0001	
C-Pitch	1.773E-08	1	1.773E-08	18.17	0.0017	
AB	0.0000	1	0.0000	39,035.39	< 0.0001	
AC	1.497E-08	1	1.497E-08	15.34	0.0029	
BC	2.813E-11	1	2.813E-11	0.0288	0.8686	
A^2	1.038E-08	1	1.038E-08	10.64	0.0085	
B^2	7.876E-06	1	7.876E-06	8070.14	< 0.0001	
C^2	1.537E-08	1	1.537E-08	15.75	0.0026	
Residual	9.759E-09	10	9.759E-10			
Lack of Fit	9.759E-09	3	3.253E-09			
Pure Error	0.0000	7	0.0000			
Cor Total	0.1152	19				

R^2 = 1.00, Mean = 0.89, Adjusted R^2 = 1.00, C.V.% = 0.0035, Predicted R^2 = 1.00, Adeq Precision = 13,351.08.

The positive coefficient for the effort arm in the fitted regression model suggests that an increase in the effort arm will increase the Mechanical Advantage, while the negative coefficient for the load arm implies that a decrease in the length of the load arm will increase Mechanical Advantage. The equation in terms of actual factors is only useful in predictions about the response for given levels of each factor. The optimization exercise for Mechanical Advantage was conducted utilizing the flexibility of the Design Expert optimization tool function. Eq. (14) was solved for the best solutions. A usual approach which involves selecting the best solution was adopted and the chosen optimal solutions gave effort arm (mm) = 67.50, load arm (mm) = 66.38 and pitch (mm) = 2.50. Standard design processes were then performed using the optimal result of the numerical optimization executed by Design expert software. Computer aided models was then used to present the physical systems.

3.2. Computer Aided Design (CAD) model

A CAD model of the universal ball joint separator using optimal conditions was first created with the aid of SolidWorks® Software. All the parts of the ball joint separator are designed in SolidWorks® individually and these parts are then assembled by applying the constraint conditions. The Fig. 4(a–d) shows different views of the bottom half of the separator while Fig. 5(a–c) show all the different views of the top half of the separator. The assembly of these different parts to form a complete model is shown in Fig. 6.

3.3. Material selection and ranking

As it can be seen from bubble chart graphs shown in Fig. 7, Young's modulus was plotted against density using the GRANTA material selec-

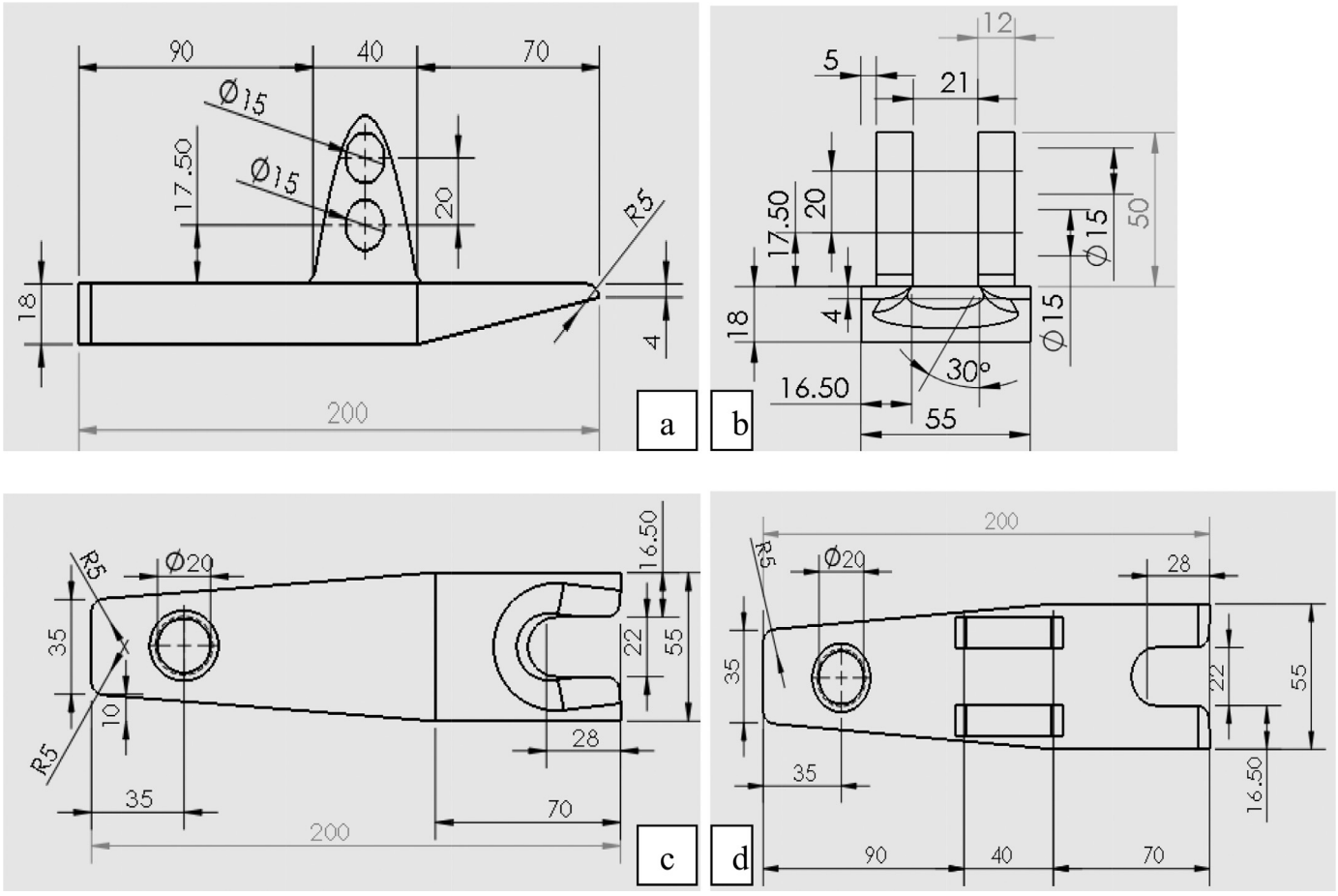

Fig. 4. Computer Aided Design of the bottom half of the separator showing (a) front view, (b) end view (c) top view (d) bottom view.

Table 2
Candidate materials screening index for ball joint separator.

	Poisson's ratio	Young's modulus (GPa)	Density (kg/m^3)	Yield Strength (MPa)	$M = \frac{E^{1/2}}{\rho}$	$M = \frac{\sigma_y{}^{1/2}}{\rho}$
Low carbon steel	0.29	207.5	7850	322.5	0.00183	0.00228
Cast iron	0.27	109	7150	280	0.00146	0.00234
High carbon steel	0.28	207.5	7850	780	0.00183	0.00355

tor. The properties were arrived at as the result of the function, objective and constraint considering large values of material index with respect to stiffness in Eq. (12) and with respect to strength in Eq. (13). With these properties, efforts were made to select a candidate material with moderate strength at low weight. Going by these properties the following materials are suggested candidate materials: Low carbon steel, Cast iron and High carbon steel. The properties of these candidate materials are shown in Table 2.

Table 3
Mesh Statistics for universal ball joint separator model.

Component	Nodes	Elements	Standard Deviation
Pivot	68,484	30,547	0.1393
Fork Half	226,209	101,534	0.1704
Bottom Half	43,112	19,054	0.1493

3.4. FEA mesh

For Finite Element Analysis (FEA), assembly drawing of the universal ball joint separator was imported in ANSYS 15.0 and the boundary conditions were applied to the model. Material properties of low carbon steel, cast iron and high carbon steel from Table 2 were assigned independently to the universal ball joint separator model. In this study, FEA mesh representing the nodes and elements for structural calculations was generated on 3D CAD model of the universal ball joint separator and the geometric model was subdivided into discrete elements. Meshing of the model was done using a tetrahedron element comprising of 151,135 elements and 337,805 nodes. The stated element type was chosen since it has a higher accuracy compared to its equivalent lesser node element. FEA mesh was generated using the auto-mesh generation algorithm in FEA software ANSYS® [28]. Mesh refinement was performed in desired segments of the device to avoid unrealistic stress concentration points [29]. Furthermore regions exposed to crack and regions of higher gradients were meshed with more element numbers when compared with other parts to magnify the accuracy of results as shown in Fig. 8. Mesh sensitivity analysis was also carried out to ensure the quality of results. The overall mesh statistics is presented in Table 3: The structural response, such as deformations, equivalent Von-Mises stresses

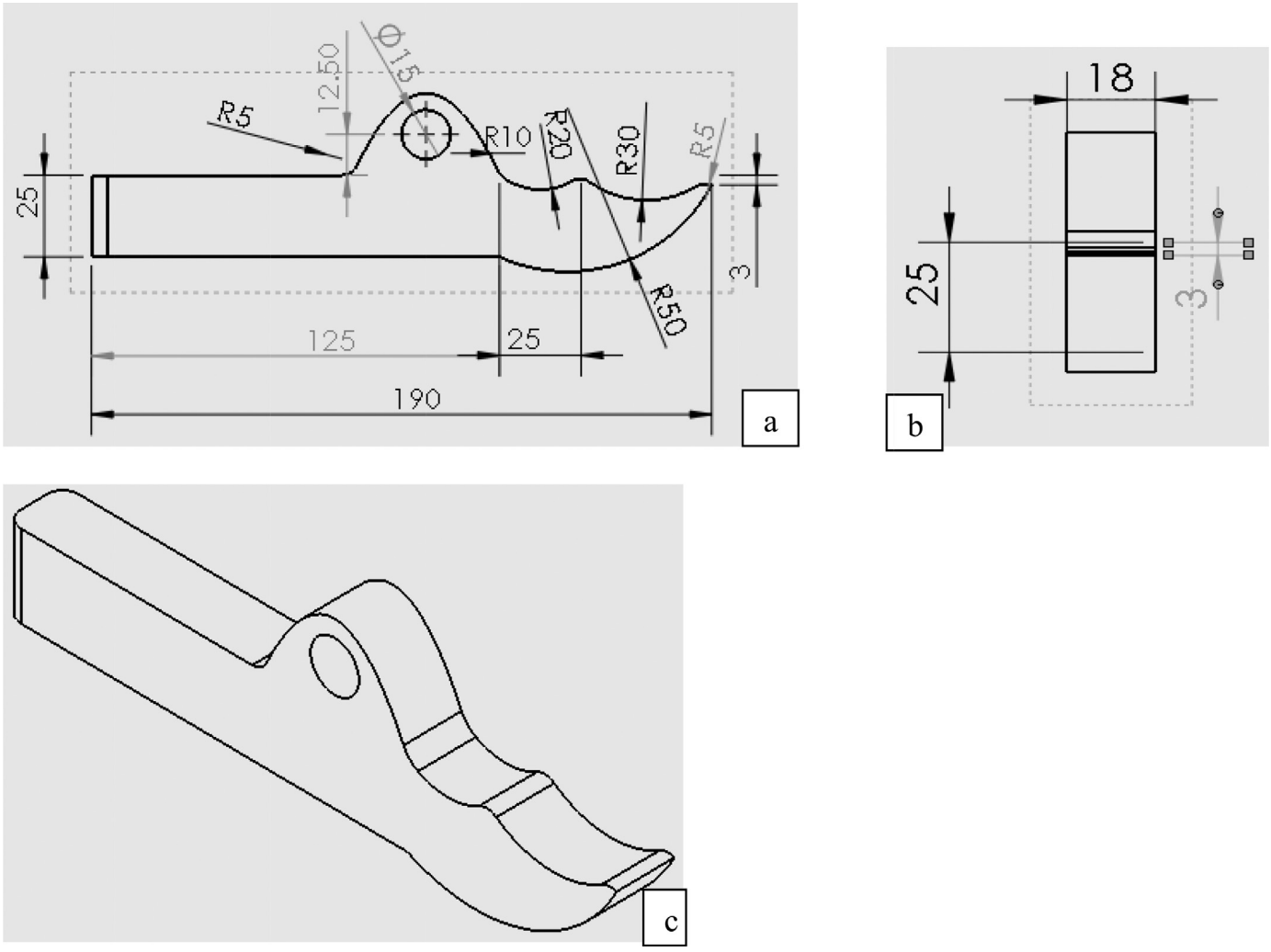

Fig. 5. Computer Aided Design of the top half of the separator showing (a) top view, (b) end view (c) isometric view.

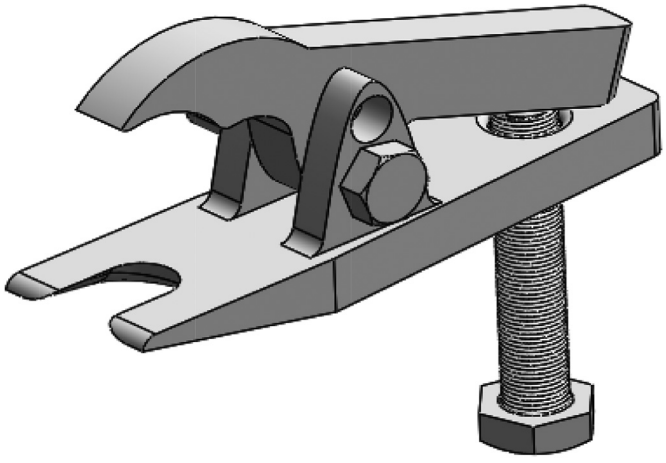

Fig. 6. Assembly Drawing of the Separator.

and principal stresses are computed and presented in Table 4 for high carbon steel.

Three different materials (low carbon steel, cast iron and high carbon steel) were further simulated using a load range of 200–1400 N which covers the average load of 500 N necessary for the removal of a ball joint [1]. The loads were applied at the exact location during a typical ball joint separation process and the results are shown in Figs. 9–11. It was seen in Figs. 9–11 that the maximum deformation occurs at the tip of the top part of the ball joint separator which is the part that comes in direct contact with the nut of the ball joint in practice.

From Figs. 9–11, it can be seen that the deformation of cast iron as compared to the other two materials is very high. Cast iron is also a brittle material which should not be subjected to high deformation to avoid failure. Low carbon steel and High Carbon steel still show similar results for the range of loads applied as their high values of yield strength enabled them to resist deformation. Although both mild steel and high carbon steel would be suitable for the production of this tool, high carbon steel is selected as the material for the production of the universal ball joint separator on the basis of strength and stability.

At the design load of 1 kN, the von-mises stress has increased to a considerable level, but it is still far below the yield stress of the material signalling no fear of sudden failure. The observed deformation is also minimal to cause a crack in the material selected [13]. The maximum stress occurs close to the pivot at the base of the bottom half. The stress however is less than the yield stress of the material and the separator would perform the required function without failure. Table 4 gave the force-stress-strain relationships of FEA model.

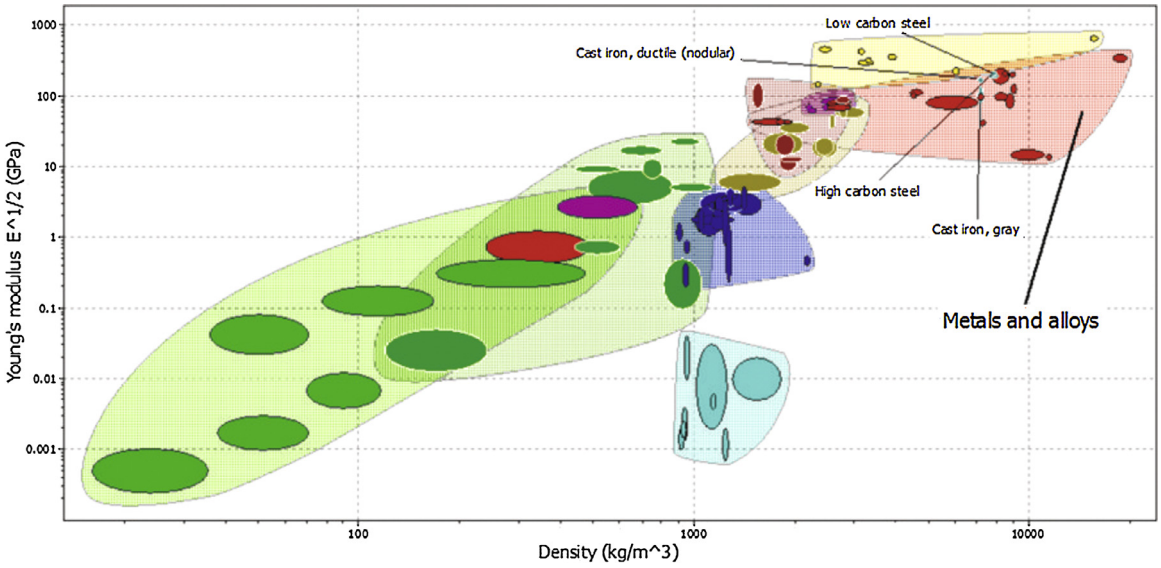

Fig. 7. Material selection chart for ball joint separator on the basis of stiffness.

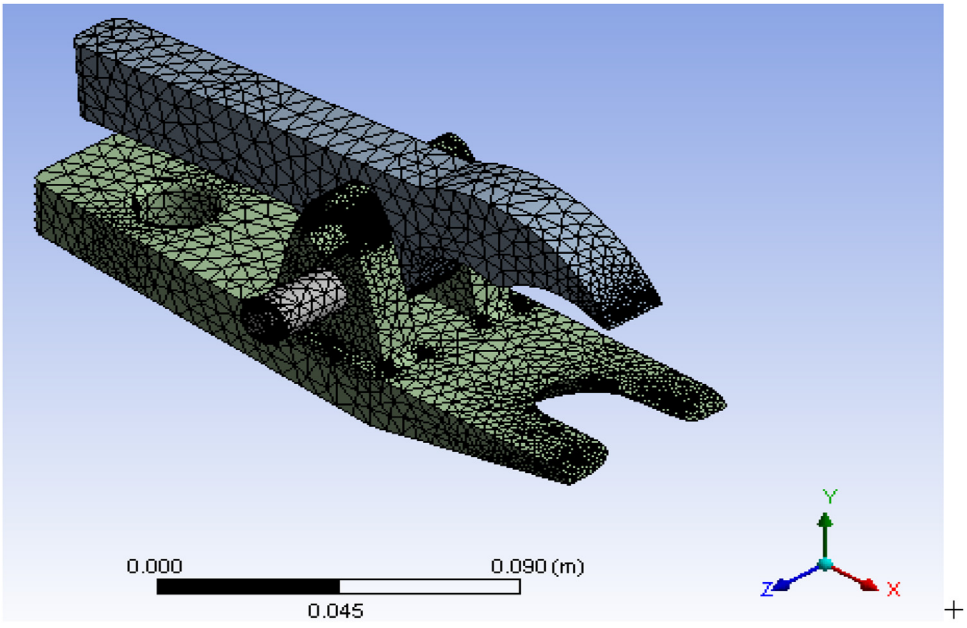

Fig. 8. Meshing of the universal ball joint separator.

Table 4
Analysis of High Carbon Steel.

S/N	Force (N)	Max Von-Mises Stress (MPa)	Max Total Deformation	Max Principal Stress (MPa)	Max Principal Strain
1	200	16.71	1.92e−5	20.51	8.84e−5
2	400	33.22	3.80e−5	40.75	1.75e−4
3	600	49.82	5.70e−5	61.11	2.63e−4
4	800	66.66	7.61e−5	81.76	3.52e−4
5	1000	83.32	9.52e−5	102.21	4.40e−4
6	1200	100.71	1.22e−4	120.89	5.38e−4
7	1400	116.73	1.33e−4	143.19	6.17e−4

3.5. Analysis of the bolt for compressive force

The results of response surface optimization gave the thread pitch of 2.5 which corresponds to M20 ISO metric thread. M20 hexagonal head bolt was therefore selected and with the aid of the ANSYS CAD software, the bolt analysis was carried out and the results are displayed in Table 5 and Fig. 12.

The results indicate that the M20 bolt would be suitable for the device as it is not approaching its yield strength of mild steel and the deformation is very negligible.

3.6. Experimental implementation

The universal ball joint separator was mounted as illustrated in Fig. 13 and it proved highly effective in the separation of the ball joint

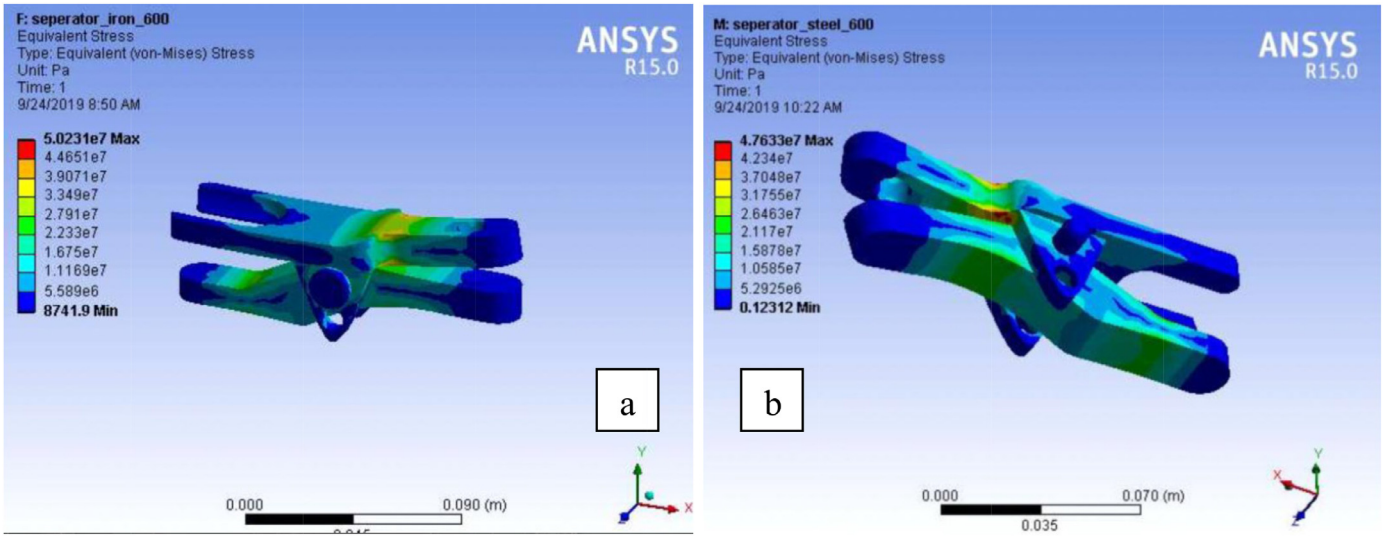

Fig. 9. Von-Mises stress at 600 N for (a) cast iron and (b) low carbon steel.

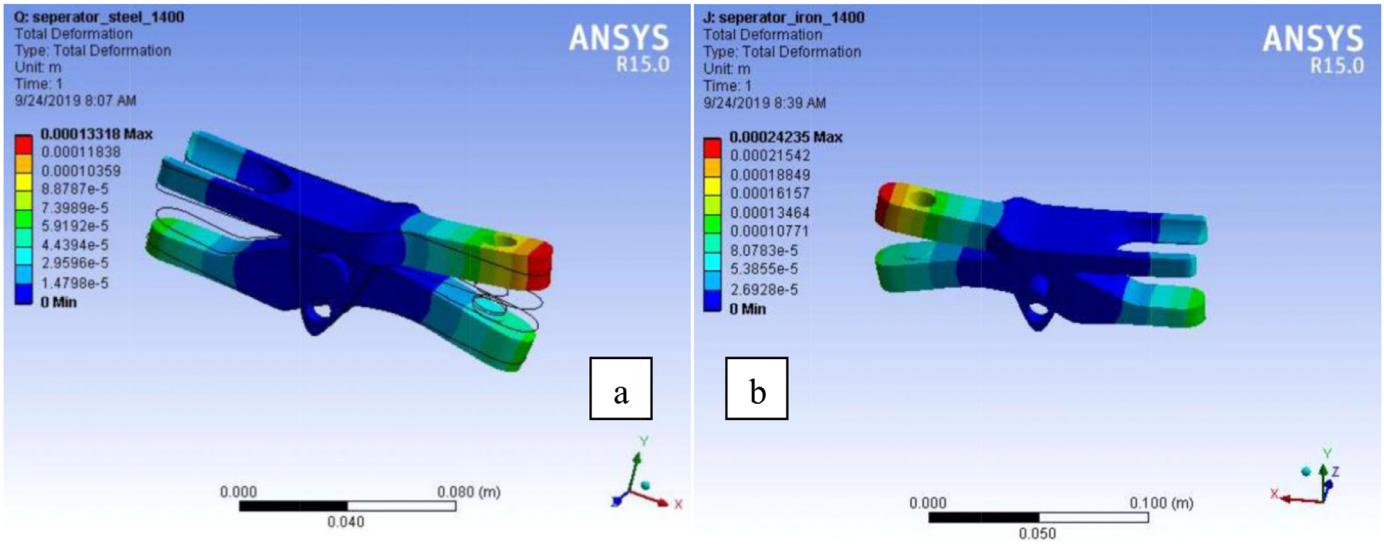

Fig. 10. Deformation analysis at 1400 N for (a) low carbon steel and (b) cast iron.

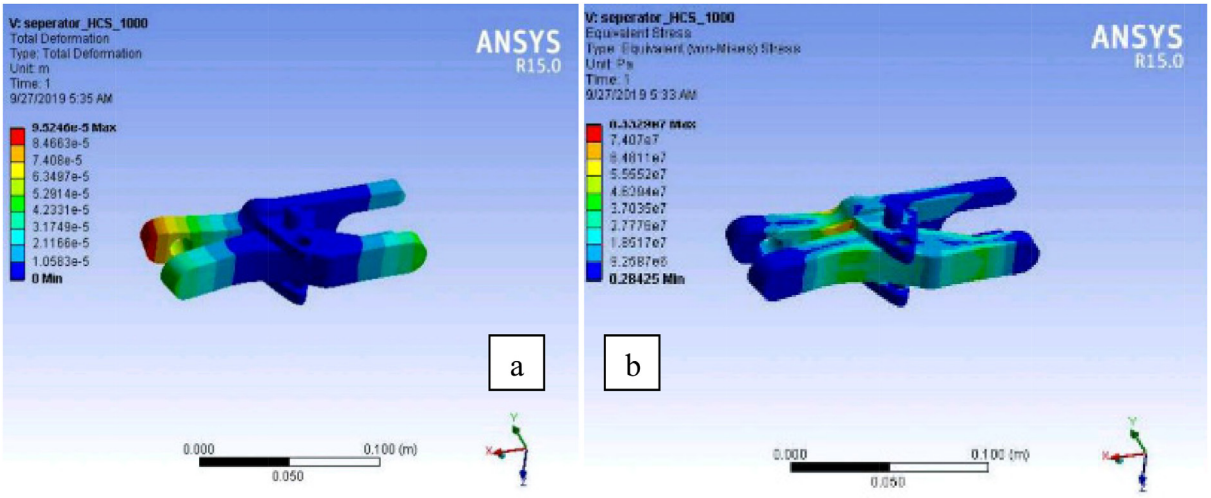

Fig. 11. (a) Deformation and (b) Von-Mises analysis for high carbon steel at 1000 N.

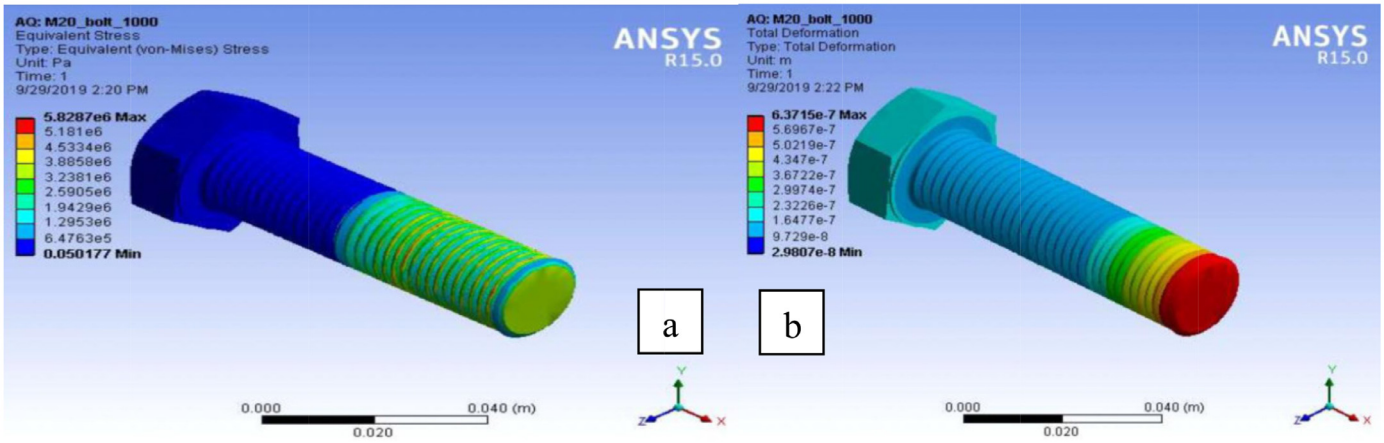

Fig. 12. Von-Mises Stress (a) and deformation (b) of M20 Bolt at load of 1000 N.

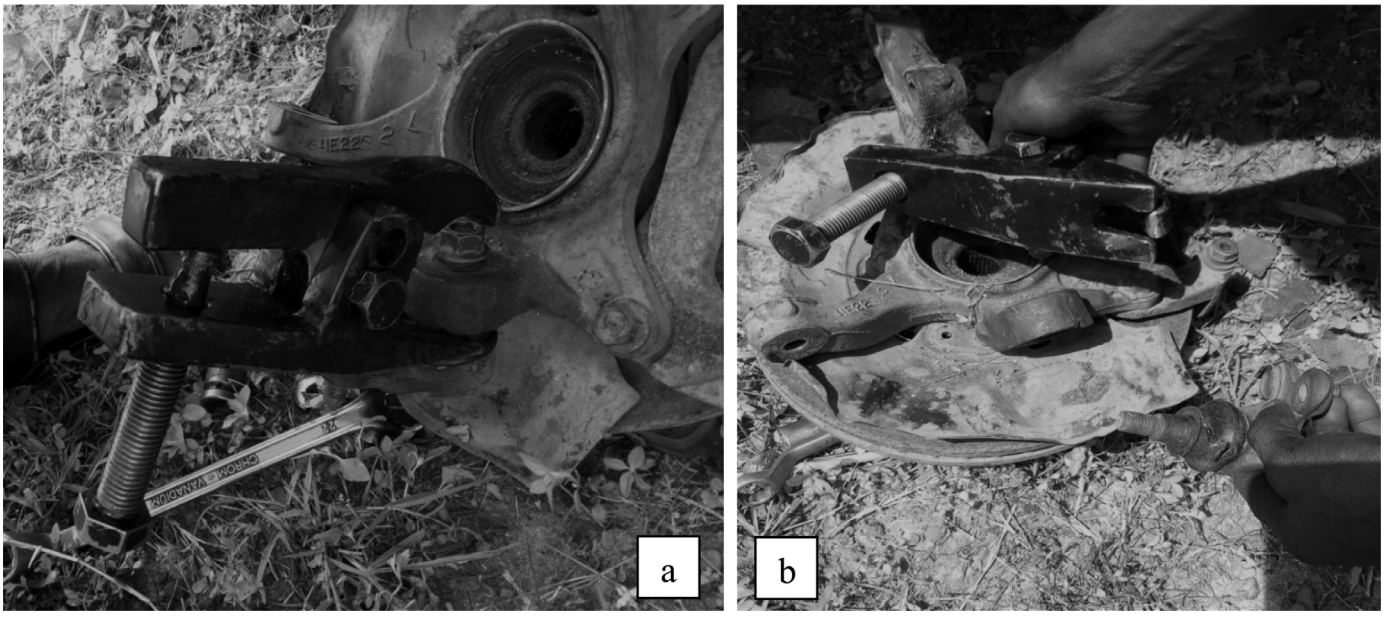

Fig. 13. Ball Joint Separation with the Universal Ball Joint Separator before (a) and after (b) separation.

Table 5
Analysis of the M20 bolt.

S/N	Force(N)	Max Von-Mises Stress (MPa)	Max Total Deformation (mm)
1	200	1.21	1.21e−7
2	400	2.43	2.05e−7
3	600	3.73	3.79e−7
4	800	4.85	4.75e−7
5	1000	5.82	6.37e−7
6	1200	7.17	6.95e−7
7	1400	8.42	8.71e−7

Table 6
Device performance features at different load levels.

S/N	W(N)	P_n(N)	M.A(-)	T(Nm)	e_b(%)	e_d(%)
1	200	235.29	0.85	256.98	30.96	83.51
2	400	470.59	0.85	513.95	30.96	83.51
3	600	705.88	0.85	770.93	30.96	83.51
4	800	941.18	0.85	1027.91	30.96	83.51
5	1000	1176.47	0.85	1284.88	30.96	83.51
6	1200	1411.76	0.85	1541.86	30.96	83.51
7	1400	1647.06	0.85	1798.84	30.96	83.51

from the steering knuckle of vehicles. The ball joints of three different car models were successfully separated and the relationship curves between torque and load were drawn according to test results in Figs. 14 and 15. The results portrayed an approximate linear relationship between the applied torque and load which is similar to the theoretical results shown in Table 6. However, it was difficult to achieve totally linear relationship for torque-load in practice because of the scattering, vulnerability, and estimation mistake that exists in the fixing procedure.

Majority of engineering devices fail to perform intended purposes due to poor lubrication of contacting surfaces [30]. Adequate lubrication has been advocated in this study to thin down the torque needed to overcome the frictional resistance of contact surfaces as captured in Figs. 14–16. Replacing the manual boll joint separation process with the use of the universal boll joint separator will likely increase productivity by reducing the tightening time and operator fatigue.

Fig. 16 compares the average of nut factor in relation to the device surface lubrication condition. The impact of oil condition on nut factor

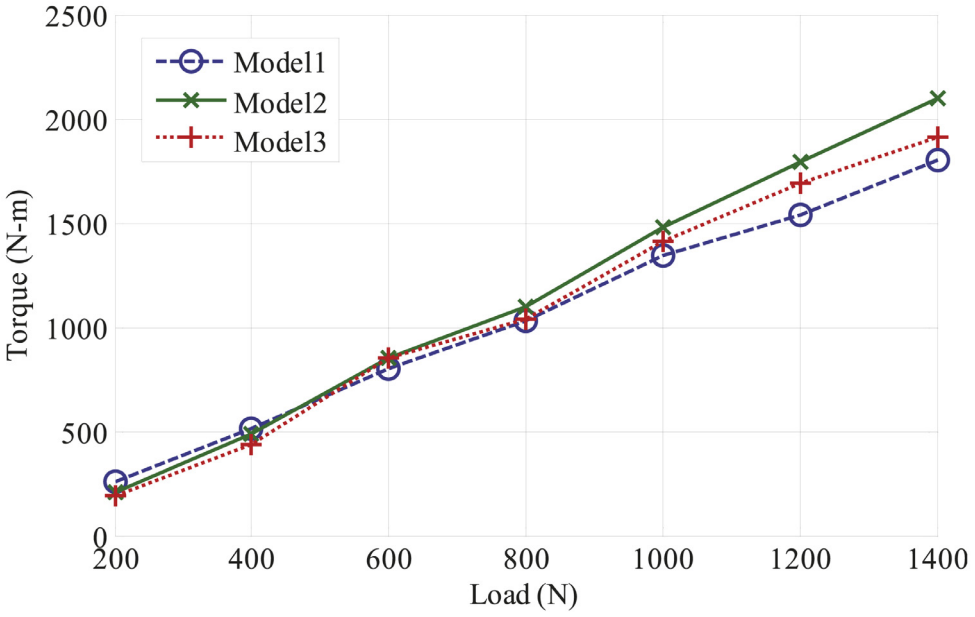

Fig. 14. Torque - load plot for three different car models when contact surfaces are lubricated.

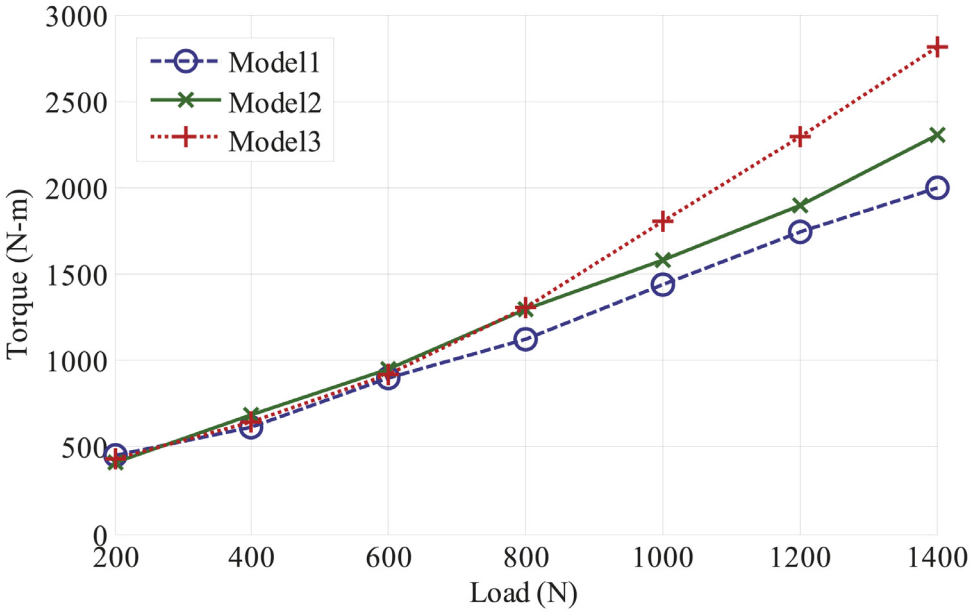

Fig. 15. Torque - load plot for three different car models when contact surfaces are not lubricated.

is accomplished by influencing the friction coefficient of contact surfaces. When the bolt contact surfaces are lubricated, the surface friction coefficient becomes smaller. Therefore, a smaller torque is needed to overcome the frictional resistance of contact surfaces as can be seen in Figs. 14 and 15. A similar outcome was also recorded in Fig. 16 as the nut factor for the lubrication condition is less compared to the non-lubricated condition. The lubrication of contact surfaces has a larger influence on the nut factor; this, according to Neethu, Sankaravelayutham and Rajeev [31] is because the nut factor varied with coating, threading tolerance, surface roughness, lubrication and material selection.

4. Conclusions

Based on the successful design, analysis and fabrication of the universal ball joint separator, the following conclusions are drawn:

- This tool effectively separated the ball joint from the steering knuckle of three different vehicles without damage to any other part while reducing the time spent in the whole separation process.
- The three design variables that affect the performance of a ball joint separator were established and the optimal solution was reported. This new improvement offers the automotive mechanics an alternative ball joint remover which can help reduce the drudgery and risk associated with the conventional ball joint separation process.
- A robust adaptation of the embodiments of existing separators leading to changes in material requirements improved the mechanical advantage and overall device efficiency in relation to the design intent.
- Considering the critical role of ball joints in providing universal pivoting movement between the wheel hubs and control arms, adequate lubrication has been advocated to thin down the torque needed to

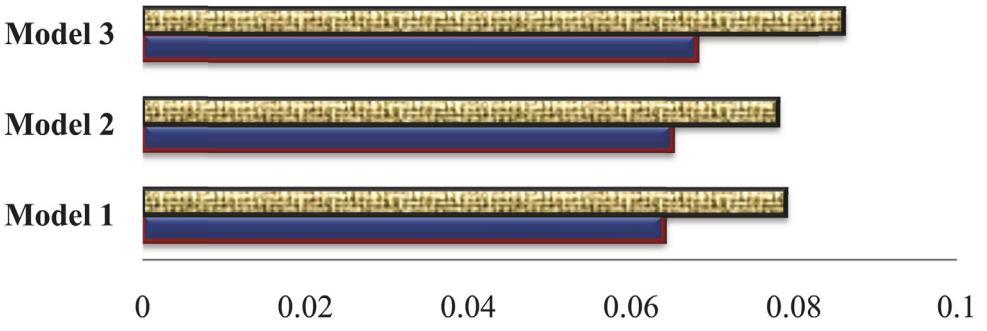

	Model 1	Model 2	Model 3
NON-LUBRICATED	0.079	0.078	0.086
LUBRICATED	0.064	0.065	0.068

Fig. 16. The influence of lubrication on Nut Factor in three different car models.

overcome the frictional resistance of contact surfaces during ball joint separation process.

References

[1] I. Muscă, I.C. Romănu, A. Gagea, Preliminary study of friction in automotive ball joints, in: IOP Conference Series: Materials Science and Engineering (Vol. 724, No. 1, IOP Publishing, 2020, p. 01, doi:10.1088/1757-899X/724/1/012020. DOI:.

[2] B.S. Sin, K.H... Lee, Process design of a ball joint, considering caulking and pull-out strength, Sci. World J. (2014), doi:10.1155/2014/971679.

[3] B.H. Jang, K.H. Lee, Analysis and design of a ball joint, considering manufacturing process, Proc. Inst. Mech. Eng. Part C 228 (2014) 146–151, doi:10.1177/0954406213497317.

[4] S.C. Hwang, K.H. Lee, Structural dynamic analysis of a ball joint, in: AIP Conference Proceedings American Institute of Physics, 1499, 2012, pp. 394–398. https://doi.org/10.1063/1.4769019.

[5] C.A. McMahon, C... Draper, Patterns of design and development in adaptive design: how do we match design method to design circumstance? DS 29: Proceedings of EDIProD 2002 (2002) 65–72 https://www.designsociety.org/publication/27322/Patterns±of±Design±and±Development±in±Adaptive±Design%3A±How±Do±We±Match±Design±Method±to±Design±Circumstance%3F.

[6] S.M. O'Shaughnessy, M.J. Deasy, J.V. Doyle, A.J. Robinson, Adaptive design of a prototype electricity-producing biomass cooking stove, Energy Sustain. Dev. 28 (2015) 41–51, doi:10.1016/j.esd.2015.06.005.

[7] G. Schuh, J.P. Prote, M. Luckert, F. Basse, V. Thomson, W. Mazurek, Adaptive design of engineering change management in highly iterative product development, Procedia CIRP 70 (2018) 72–77, doi:10.1016/j.procir.2018.02.016.

[8] C.O.A. Agbo, Adaptive design and performance evaluation of compact acoustic enclosures built with GFRP for portable mini-generators, J. Eng. Res. Rep. (2019) 1–11, doi:10.9734/jerr/2019/v7i316972.

[9] P.V. Balachandran, D. Xue, J. Theiler, J. Hogden, T. Lookman, Adaptive strategies for materials design using uncertainties, Sci. Rep. 6 (2016) Article 19660, doi:10.1038/srep19660.

[10] Y.C. Tian, H.E. Fei, X. Zhang, Adaptive design of shield radius for open type hard rock TBM, J. ZheJiang Univ. 53 (12) (2019) 2280–2288, doi:10.3785/j.issn.1008-973X.2019.12.004.

[11] E. Sariyildiz, K Ohnishi, An adaptive reaction force observer design, IEEE/ASME Trans. Mech. 20 (2014) 750–760, doi:10.1109/TMECH.2014.2321014.

[12] G. Pahl, W. Beitz, Feldhusen J., K.-.H. Grote, Engineering Design a Systematic Approach, third ed., Springer-Verlag London Limited, 2007, doi:10.1007/978-1-84628-319-2.

[13] C.A. Alumkal, G.P. Rao, V.M. Pillai, Analysis of robust and adaptive designs for dynamic part population, Int. J. Bus. Perform. Supply Chain Model. 3 (2011) 124–140, doi:10.1504/IJBPSCM.2011.041375.

[14] A.K. Goel, E. Stroulia, Functional device models and model-based diagnosis in adaptive design, AI EDAM 10 (1996) 355–370 https://doi.org/10.1017/S0890060400001670.

[15] A. Nakao, H. Kaneko, K. Funatsu, Development of an adaptive experimental design method based on probability of achieving a target range through parallel experiments, Ind. Eng. Chem. Res. 55 (2016) 5726–5735, doi:10.1021/acs.iecr.6b00852.

[16] B.C. B. Ramos, P. Melgosa, P. Castrillo, The importance of adaptive expertise in CAD learning: maintaining design intent, J. Eng. Des. 29 (2018) 569–595, doi:10.1080/09544828.2018.1519183.

[17] G. Irsel, Computer aided adaptive system design with engineering systematics and manufacturing, Adv. Sci. Technol. Res. J. (2017) 11, doi:10.12913/22998624/77069.

[18] F. Karaçam, T. Timarci, Stacking sequence optimization of composite beams with different layer thicknesses, Adv. Sci. Technol. Res. J. 9 (2015) 7–11, doi:10.12913/22998624/2358.

[19] J. Arup, Adaptive design on crank and slotted lever mechanism, ADBU J. Eng. Technol. 4 (2016) http://journals.dbuniversity.ac.in/ojs/index.php/AJET/article/view/195.

[20] P.C. Jagdish, G.C. Poonam, M.K. Kedar, Design and fabrication of lever operated wheelchair for disabled person with no legs, Int. Adv. Res. J. Sci. Eng. Technol. 6 (2019) 66–70, doi:10.17148/IARJSET.2019.6111.

[21] R. Ardan, Mastication force analysis on the fulcrum point of first class lever on lower jaw distal free end denture, Padjadjaran J. Dentistry 20 (2008) 49–52, doi:10.24198/pjd.vol20no1.14153.

[22] A.A. Kumbhar, V.R. Gambhire, Experimental testing of toggle lever caliper cable trolley brake for fail safe, Int. J. Res. IT Manag. Eng. 6 (2016) 31–36 http://www.indusedu.org/pdfs/IJRIME/IJRIME_916_38361.pdf.

[23] S.R. Schmid, B.J. Hamrock, B.O. Jacobson, Fundamentals of Machine elements: SI Version, CRC Press, 2014.

[24] J. Bickford, Handbook of Bolts and Bolted Joints, CRC Press, Boca Raton, FL, 1998.

[25] D.D. Aaron, J.M. Walter, E.E. Wilson, Machine Design – Theory and Practice, Macmillian Pub. Co, New York, 1975.

[26] M. Ashby, F Materials Selection in Mechanical Design, fourth ed., Butterworth-Heinemann, 2011.

[27] C.C. Ihueze, A.E. Oluleye, C.E. Okafor, C.M. Obele, J. Abdulrahman, S. Obuka, R Ajemba, Plantain fibre particle reinforced HDPE (PFPRHDPE) for gas line piping design, Int. J. Plast. Technol. 21 (2017) 370–396, doi:10.1007/s12588-017-9191-6.

[28] T. Stolarski, Y. Nakasone, S. Yoshimoto, Engineering Analysis with ANSYS Software, Elsevier Science, 2011, doi:10.1016/B978-0-7506-6875-0.X5030-3.

[29] U. Mughal, H. Khawaja, M. Moatamedi, Finite element analysis of human femur bone, Int. J. Multiphys. 9 (2016), doi:10.1260/1750-9548.9.2.101.

[30] R.G. Budynas, J.K. Nisbett, Shigley's Mechanical Engineering Design, 10th ed., McGraw-Hill Education, 2015.

[31] P. Neethu, P. Sankaravelayutham, N Rajeev, Nut factor analysis of aluminium IVD coated and cadmium electroplated high strength fasteners, Int. Res. J. Eng. Technol. 4 (2017) 807–809, https://www.irjet.net/archives/V4/i6/IRJET-V4I6137.pdf.